

Charge trapping characteristics of  
Al<sub>2</sub>O<sub>3</sub>/Al-rich Al<sub>2</sub>O<sub>3</sub>/SiO<sub>2</sub> stacked films  
fabricated by radio-frequency magnetron  
co-sputtering

著者	Nakata Shunji, Maeda Ryoji, Kawae Takeshi, Morimoto Akiharu, Shimizu Tatsuo
journal or publication title	Thin Solid Films
volume	520
number	3
page range	1091-1095
year	2011-11-30
URL	<a href="http://hdl.handle.net/2297/30118">http://hdl.handle.net/2297/30118</a>

doi: 10.1016/j.tsf.2011.08.011

## Charge Trapping Characteristics of Al<sub>2</sub>O<sub>3</sub>/Al-rich Al<sub>2</sub>O<sub>3</sub>/SiO<sub>2</sub> Stacked Films Fabricated by Radio-Frequency Magnetron Co-Sputtering

Shunji Nakata <sup>a,\*</sup>, Ryoji Maeda <sup>b</sup>, Takeshi Kawae <sup>b</sup>, Akiharu Morimoto <sup>b</sup>,  
Tatsuo Shimizu <sup>b</sup>

<sup>a</sup> NTT Microsystem Integration Labs., Atsugi, Kanagawa 243-0198, Japan

<sup>b</sup> Kanazawa University, Kakuma, Kanazawa, 920-1192, Japan

\*Corresponding author. Tel.: +81 462402858. E-mail: nakata.shunji@lab.ntt.co.jp

A thin-film structure comprising Al<sub>2</sub>O<sub>3</sub>/Al-rich Al<sub>2</sub>O<sub>3</sub>/SiO<sub>2</sub> was fabricated on Si substrate. We used radio-frequency magnetron co-sputtering with Al metal plates set on an Al<sub>2</sub>O<sub>3</sub> target to fabricate the Al-rich Al<sub>2</sub>O<sub>3</sub> thin film, which is used as a charge storage layer for nonvolatile Al<sub>2</sub>O<sub>3</sub> memory. We investigated the charge trapping characteristics of the film. When the applied voltage between the gate and the substrate is increased, the hysteresis window of capacitance-voltage (C-V) characteristics becomes larger, which is caused by the charge trapping in the film. For a fabricated Al-O capacitor structure, we clarified experimentally that the maximum capacitance in the C-V hysteresis agrees well with the series capacitance of insulators and that the minimum capacitance agrees well with the series capacitance of the semiconductor depletion layer and stacked insulator. When the Al content in the Al-rich Al<sub>2</sub>O<sub>3</sub> is increased, a large charge trap density is obtained. When the Al content in the Al-O is changed from 40 to 58 %, the charge trap density increases from 0 to  $18 \times 10^{18} \text{ cm}^{-3}$ , which is 2.6 times larger than that of the trap memory using SiN as the charge storage layer. The device structure would be promising for low-cost nonvolatile memory.

*Key words:* radio-frequency magnetron sputtering, oxide, Al-rich Al<sub>2</sub>O<sub>3</sub>/SiO<sub>2</sub> interface, charge trap, C-V hysteresis, MIS theory

## 1. Introduction

Nanoscale devices have been widely studied [1-5] for large-scale integration. In particular, TaN-Al<sub>2</sub>O<sub>3</sub>-SiN-oxide-silicon trap memory devices [3-5] have been attracting increasing attention because they are expected to offer extremely large-scale integration due to their thin tunnel insulator (SiO<sub>2</sub>) and thin block insulator (Al<sub>2</sub>O<sub>3</sub>).

Recently, we proposed a simplified trap memory that uses Al<sub>2</sub>O<sub>3</sub> for the tunnelling insulator and blocking insulator and Al-rich Al<sub>2</sub>O<sub>3</sub> for the charge storage layer. We clarified that the structure is very effective for nanoscale devices due to its simple structure and thin insulator [6-9]. However, a concern for this device is the interface between the Al<sub>2</sub>O<sub>3</sub> and Si. It has been reported that defects near the interface degrade the mobility in field-effect transistors considerably [10,11]. The low mobility causes low operation speed, which is 1/10 that of the conventional value.

In the present work, to resolve the above concern, we fabricated an Al<sub>2</sub>O<sub>3</sub>/Al-rich Al<sub>2</sub>O<sub>3</sub>/SiO<sub>2</sub>/Si structure using the radio-frequency (RF) magnetron co-sputtering method. The structure has three merits. The first is that SiO<sub>2</sub> is already very widely used as the tunnelling insulator in conventional nonvolatile memory [12] so that its use in the memory device enables us to use the prevailing process, i.e., thermal oxidation. The second is an ideal SiO<sub>2</sub>/Si interface, near which there are almost no defects so that the mobility degradation does not occur. The third is that the Al-rich Al<sub>2</sub>O<sub>3</sub> layer can produce many trap sites as pointed out previously [6-9].

For the Al<sub>2</sub>O<sub>3</sub>/Al-rich Al<sub>2</sub>O<sub>3</sub>/SiO<sub>2</sub>/Si structure, capacitance evaluation, or in other words, dielectric constant evaluation, is very important for investigating the electrical field across each layer, which is useful for analyzing band bending when programming and erasing. For the capacitance evaluation, orthodox MIS (metal-insulator-semiconductor) theory would be effective. In this article, we calculate the

insulator capacitance of each stacked film and the semiconductor depletion-layer capacitance theoretically. Using these values, we estimate the maximum and minimum capacitance in capacitance-voltage (C-V) hysteresis curves. The estimated values agree well with the experimental ones. From this analysis, the capacitance value in each layer is confirmed.

In the Al-rich Al<sub>2</sub>O<sub>3</sub> layer, how the charge trap density changes as a function of the Al content is still not fully understood. Therefore, we changed the Al content from 40 to 60 % and evaluated the charge trap density. We also examined the data retention of the film.

The rest of this paper is organized as follow. Section 2 presents experimental procedures for the film. Section 3 describes the experimental results, which includes the film deposition characteristics (the Al content and leakage current density), C-V characteristics, charge trap density, and data retention. Conclusions are finally described in Section 4.

## 2. Experiment

In this experiment, we used (100) n-type Si wafers ( $\rho \cong 1.5 \times 10^{-2} \Omega \text{ cm}$ .) as substrates. As shown in Fig. 1(a), 2.0 nm of SiO<sub>2</sub> was first formed as a tunnel barrier insulator by thermal oxidation. Next, 5.4 nm of Al-rich Al<sub>2</sub>O<sub>3</sub> was deposited as a charge storage layer by the co-sputtering method. Finally, 7.3 nm of stoichiometric Al<sub>2</sub>O<sub>3</sub> was deposited as the blocking barrier insulator by conventional RF sputtering. The sample was annealed at 200 °C for 1 hour effectively during deposition because the substrate temperature was set at 200 °C. In this experiment, annealing at 550 °C as in ref. 9 was not performed after the Al<sub>2</sub>O<sub>3</sub> blocking layer was deposited. A gate electrode with a diameter of 100  $\mu\text{m}$  was formed by thermal evaporation of Al. The

band diagram of this structure is shown in Fig. 1(b). Al<sub>2</sub>O<sub>3</sub> has a 2.8-eV conduction barrier height [13]. In Al-rich Al<sub>2</sub>O<sub>3</sub>, the localized level is thought to be about 2.4 eV from the conduction band [14]. Regarding conduction band offsets, the band diagram in Fig. 1(b) is not accepted universally. There is an experimental report that shows much lower values in the case of an ultrathin layer [15]. The conduction band offsets of the ultrathin layer is an important issue. Much research will be necessary to clarify this point.

Here, we explain the co-sputtering method. For the fabrication of Al-rich Al<sub>2</sub>O<sub>3</sub>, we used RF magnetron co-sputtering equipment [9]. During co-sputtering, Al metal plates (plate size: 2 cm×0.5 cm) were set on the Al<sub>2</sub>O<sub>3</sub> target, which had a diameter of 9.2 cm. The Al content of the Al-O film can be controlled by changing the areal ratio of the Al metal on the target. A schematic representation of the co-sputtering system is shown in Fig. 2, where (a) and (b) are cross-sectional and top views, respectively. Atoms are sputtered from a target and reach wafers as shown in Fig. 2(a). The ratio of sputtered atoms from the target is determined by the ratio of Al plate area in the erosion region area in Fig. 2(b).

During deposition of Al<sub>2</sub>O<sub>3</sub> and Al-rich Al<sub>2</sub>O<sub>3</sub>, Ar gas was used for sputtering. RF frequency was 13.56 MHz. The distance between the target electrode and substrate electrode was about 4 cm. After deposition, the deposited film thickness was measured with a spectroscopic ellipsometer. To investigate the Al content in the Al-O film, we used an electron probe micro-analyzer, which allows us to evaluate the Al content non-destructively by radiating an electron beam to the sample. Acceleration voltage and sample current were 15 kV and 20 nA, respectively. Beam size was 30 μm.

Electrical measurements were performed using a probe at room temperature.

Leakage current was measured with a precision semiconductor parameter analyzer (HP4156). Capacitance was measured with a precision LCR meter (HP4284A) at 1 MHz.

### 3. Results and Discussion

#### 3.1. Film deposition

First, we describe the deposition characteristics of RF-magnetron co-sputtering. Figure 3(a) shows the Al content in the Al-rich Al<sub>2</sub>O<sub>3</sub> as a function of the areal ratio of Al metal on the Al<sub>2</sub>O<sub>3</sub> target. A ratio of zero means there are no Al metal plates on the target, which corresponds to the deposition of stoichiometric Al<sub>2</sub>O<sub>3</sub>. A ratio of 100 % means the Al<sub>2</sub>O<sub>3</sub> target is completely covered with Al plates. It is clear that the Al content changes linearly as a function of the areal ratio. In the experiment, the Al content reached as high as 70 %, which can provide sufficiently Al-rich Al<sub>2</sub>O<sub>3</sub>.

The leakage current characteristics of the structure in Fig. 1 with an Al content of around 50 % are shown in Fig. 3(b). When the electric field is smaller than  $2 \times 10^8$  V/m, leakage current is on the order of  $10^{-9}$  A/cm<sup>2</sup>, which is almost the same level as that for Al-O fabricated by electron-cyclotron-resonance sputtering [16] and in our previous work [9].

#### 3.2. Capacitance-voltage characteristic

Here, we first discuss the C-V characteristic of the single Al-rich Al<sub>2</sub>O<sub>3</sub> layer with an Al content 50 % to investigate the permittivity. The sample was deposited on (100) n-type Si wafers ( $\rho \cong 5 \Omega \text{ cm}$ .) as substrates. The film thickness was 76 nm. Annealing was not performed after deposition. A gate electrode with a diameter of 200  $\mu\text{m}$  was formed by thermal evaporation of Al.

We measured the high-frequency C-V characteristics at 1 MHz at room temperature. The sweep rate was about 1 V/sec. The result is shown in Fig. 4. The voltage to the gate electrode was swept from 7 to -7 V. Next, the voltage was reversed from -7 to 7 V. Arrows in Fig. 4 show the C-V hysteresis direction.

Next, we discuss the capacitance value in Fig. 4 using MIS theory. When the maximum applied gate voltage is 7 V, the capacitance value is almost equal to insulator capacitance  $C_i$ . From Fig. 4,  $C_i$  is estimated to be about 30 pF. The  $C_i$  is the capacitance of Al-rich Al<sub>2</sub>O<sub>3</sub>. Here, we consider the dielectric constant of the insulator. Using the relation  $C=\epsilon S/d$  and the vacuum permittivity of  $8.85\times 10^{-12}$  F/m, we estimate the dielectric constant to be 8.2. From previous research [17], it is known that the dielectric constant of stoichiometric Al<sub>2</sub>O<sub>3</sub> is 8.1. Then, the dielectric constant of Al-rich Al<sub>2</sub>O<sub>3</sub> with Al content of 50 % is almost the same as that of stoichiometric Al<sub>2</sub>O<sub>3</sub>. Therefore, for easy calculation, we set the dielectric constant of stoichiometric Al<sub>2</sub>O<sub>3</sub> and Al-rich Al<sub>2</sub>O<sub>3</sub> with Al content of 50 % to be 8.

Next, we consider the minimum capacitance  $C_{min}$  when  $V=-7$  V. The  $C_{min}$  is the series capacitance of  $C_i$  and the semiconductor depletion-layer capacitance  $C_D$  (i.e.,  $1/C_{min} = 1/C_i + 1/C_D$ ). The depletion layer width of semiconductor  $W$  is calculated by the formula [18]

$$W^2 = 4\epsilon_{Si}kT / (q^2N_D) \cdot \ln(N_D / n_i), \quad (1)$$

where  $\epsilon_{Si}$  is the permittivity of Si,  $k$  is the Boltzmann constant,  $T$  is temperature,  $q$  is the elementary charge,  $N_D$  is the impurity concentration, and  $n_i$  is the intrinsic carrier density. Using the resistivity of the wafer ( $\rho \approx 5 \Omega\text{cm}$ ), we estimate  $N_D$  to be  $1 \times 10^{15} \text{ cm}^{-3}$  [18]. Using  $n_i = 1.45 \times 10^{10} \text{ cm}^{-3}$ , we have

$$\ln(N_D / n_i) = 11.1 . \quad (2)$$

Then, using  $T=20$  °C,  $q=1.6\times 10^{-19}$  C, and  $\varepsilon_{Si}=11.9\times 8.85\times 10^{-12}$  F/m, we can estimate  $W$  to be 860 nm. Then, we have

$$C_D = \frac{\varepsilon_{Si}}{W} \cdot \pi(100\mu m)^2 = 3.8 \text{ pF}. \quad (3)$$

Using  $C_i$  and  $C_D$ , we can estimate  $C_{min}$  as 3.4 pF. This value is very close to the experimental value of 3 pF.

Next, we measured the high-frequency C-V characteristics of the Al-rich Al<sub>2</sub>O<sub>3</sub> structure in Fig. 1 with an Al content of 50 % at 1 MHz at room temperature. The sweep rate was about 1 V/sec. The results are shown in Fig. 5. The maximum applied gate voltage was 1, 2, 3, 4, or 5 V. When the maximum applied gate voltage was 1 V, the voltage to the gate electrode was swept from 1 to -1 V. Next, the voltage was reversed from -1 to 1 V. We repeated this process with maximum applied gate voltages from 2 to 5 V. The hysteresis voltage window  $\Delta V$  (the difference voltage between the hysteresis at mid capacitance in C-V curves, i.e., 26pF) becomes large when the maximum applied gate voltage increases. Arrows in Fig. 5 show the C-V hysteresis direction. From this characteristic, we know that electrons or holes tunnel through the SiO<sub>2</sub>.

Figure 6(a) shows the  $\Delta V$ - $\Delta C$  plot when the maximum applied gate voltage is changed, where the  $\Delta C$  is the difference between the large and small capacitances at the gate voltage of 0V in Fig. 5. It is clear that  $\Delta V$  and  $\Delta C$  become larger when the maximum applied gate voltage increases.

Figure 6(b) shows  $\Delta V$  as a function of the maximum applied gate voltage. The  $\Delta V$  does not increase linearly. It is almost zero when the maximum applied gate voltage is around 0 V. When the maximum applied gate voltage increases,  $\Delta V$  increases rapidly. This is the same as in our previous work [8].

Next, we discuss the capacitance value in Fig. 5 using MIS theory. When the maximum applied gate voltage is 5 V, the capacitance value is almost equal to insulator capacitance  $C_i$ . From Fig. 5,  $C_i$  is estimated to be about 35 pF. The  $C_i$  is equal to the series capacitance of SiO<sub>2</sub>, Al-rich Al<sub>2</sub>O<sub>3</sub>, and Al<sub>2</sub>O<sub>3</sub> (i.e.,  $1/C_i = 1/C_{SiO_2} + 1/C_{Al-O} + 1/C_{Al_2O_3}$ ), where  $C_{SiO_2}$ ,  $C_{Al-O}$ , and  $C_{Al_2O_3}$  are the capacitances of SiO<sub>2</sub>, Al-rich Al<sub>2</sub>O<sub>3</sub>, and Al<sub>2</sub>O<sub>3</sub>, respectively. The dielectric constants of SiO<sub>2</sub> and Al<sub>2</sub>O<sub>3</sub> are 3.9 and 8, respectively. The dielectric constant of Al-rich Al<sub>2</sub>O<sub>3</sub> with Al content of 50% is 8 as discussed above. Then, we can estimate  $C_{SiO_2}$  as

$$C_{SiO_2} = \frac{3.9 \times 8.85 \times 10^{-12} \text{ F/m}}{2.0 \text{ nm}} \cdot \pi (50 \mu\text{m})^2 = 135 \text{ pF} . \quad (4)$$

Similarly, we can estimate  $C_{Al-O}$  and  $C_{Al_2O_3}$  as 103 and 76.1 pF, respectively.

Therefore, insulator capacitance  $C_i$  is estimated as

$$C_i = \frac{1}{1/C_{SiO_2} + 1/C_{Al-O} + 1/C_{Al_2O_3}} = 33.1 \text{ pF} . \quad (5)$$

This value is consistent with the experimental results.

Next, we consider the minimum capacitance  $C_{min}$  when  $V = -5$  V. The  $C_{min}$  is the series capacitance of  $C_i$  and the semiconductor depletion-layer capacitance  $C_D$ . The depletion layer width of semiconductor  $W$  is calculated by formula (1). Using the resistivity of the wafer ( $\rho \cong 1.5 \times 10^{-2} \Omega \text{ cm}$ ), we estimated  $N_D$  to be  $2 \times 10^{18} \text{ cm}^{-3}$  [18]. Using  $n_i = 1.45 \times 10^{10} \text{ cm}^{-3}$ , we have

$$\ln(N_D / n_i) = 18.7 . \quad (6)$$

Then, using the same parameters  $T$ ,  $q$ , and  $\epsilon_{Si}$ , we can estimate  $W$  to be 25 nm. Then, we have

$$C_D = \frac{\varepsilon_{Si}}{W} \cdot \pi(50\mu m)^2 = 33.1 \text{ pF}. \quad (7)$$

Using  $C_i$  and  $C_D$ , we can estimate  $C_{min}$  as 16.6 pF. This value is very close to the experimental value of 17 pF.

Therefore, in the fabricated stacked thin film, it is clarified that the dielectric constant of SiO<sub>2</sub> is 3.9 and that of stoichiometric Al<sub>2</sub>O<sub>3</sub> and Al-rich Al<sub>2</sub>O<sub>3</sub> with Al content of 50 % is 8.

### 3.3. Charge trap density

Next, we discuss the charge trap density in the Al-rich Al<sub>2</sub>O<sub>3</sub> film. The stored charge per unit area  $\Delta Q$  can be evaluated as  $\Delta Q = C_b \Delta V / 2$ , where  $C_b$  is the capacitance per unit area of the blocking barrier insulator [19]. The  $C_b$  is written as  $C_b = \varepsilon / d_b$ , where  $d_b$  is the blocking insulator's thickness and  $\varepsilon$  is its permittivity. Then, we can estimate  $d_b$  as  $7.3 + 5.4 / 2 = 10$  nm. The  $\varepsilon$  is  $8 \times 8.85 \times 10^{-12}$  F/m. Then,  $C_b$  is estimated to be  $7.08 \times 10^{-3}$  F·m<sup>-2</sup>. Since  $\Delta V$  is 2.9 V when the maximum applied gate voltage is 5 V,  $\Delta Q$  of the Al-rich Al<sub>2</sub>O<sub>3</sub> memory is estimated to be  $10.3 \times 10^{-7}$  C·cm<sup>-2</sup>, so that the electron trap density [ $N_e = \Delta Q / (5.4 \text{ nm} \times 1.6 \times 10^{-19} \text{ C})$ ] is estimated to be  $11.9 \times 10^{18}$  cm<sup>-3</sup>. This value is larger than that of metal-nitride-oxide-silicon, which is  $7 \times 10^{18}$  [cm<sup>-3</sup>] [19].

Next, we investigate the charge trap density as a function of Al content. The results are shown in Fig. 7. In the experiment, the gate voltage of 5 or -5 V was applied for 1 sec. The charge trap density is almost 0 when Al content is 40 % (stoichiometric Al<sub>2</sub>O<sub>3</sub>). When Al content increases, the charge trap density increases.

When the Al content is 58 %, the charge trap density reaches  $18 \times 10^{18}$  cm<sup>-3</sup>. This

value is larger than the previous values ( $8.1 \times 10^{18} \text{ cm}^{-3}$  in ref. 7 and  $14.4 \times 10^{18} \text{ cm}^{-3}$  in ref. 8). It is expected that the more the Al content increases, the larger the charge trap density becomes. When memory cell size is 10-nm square and the charge trap layer is 2-nm thick, we estimate the number of trapped electrons to be 3.6 using the charge trap density of  $18 \times 10^{18} \text{ cm}^{-3}$ . In the conventional silicon-oxide-nitride-oxide-silicon trap memory, the average number of trapped electrons is estimated to be only 1.4 by using the charge trap density of  $7 \times 10^{18} \text{ cm}^{-3}$ . Moreover, due to the statistical fluctuation, traps can not exist in many cells. However, with Al-rich Al<sub>2</sub>O<sub>3</sub>, we can easily realize the situation with many trap sites because Al-rich Al<sub>2</sub>O<sub>3</sub> maintains its nonstoichiometric characteristic even at the atomic level (1-nm order). The total change in the number of electrons in the Al-rich Al<sub>2</sub>O<sub>3</sub> layer during injection and ejection is 7.2, which corresponds to the change of not  $\Delta V/2$  but of  $\Delta V$ . This value is consistent with that in the previous consideration [7].

#### 3.4. Data Retention

Finally, we measured the data retention. The measurement temperature was 20 °C. The data retention for the samples with Al content of 50 % is shown in Fig. 8. First, we applied 5 V to the gate for 1 sec and measured the capacitance value as a function of time under gate voltage of 0 V (H in Fig. 8). After measuring H data, we applied -5 V to the gate for 1 sec and measured it again under gate voltage of 0 V (L in Fig. 8). The capacitance value changes gradually because the thickness of SiO<sub>2</sub> is comparatively small (2 nm). However, if the thickness increases by 1 nm, the leakage current would decrease to 1/1000 so that the slope of the capacitance change would decrease to 1/1000 [10,11]. Therefore, it is expected that the device could store data for more than  $3 \times 10^8$  s by increasing the thickness of SiO<sub>2</sub> to 3 nm.

Figure 9 shows the data retention for the samples with Al content of 58 %. In this case, the retention characteristic is not better than that in Fig. 8. For this sample, the thickness of SiO<sub>2</sub> should be increased to 4 nm, an increase of 1 nm from 3 nm. By increasing SiO<sub>2</sub> thickness, it is also expected that the sample with Al content of 58 % could store data for more than  $3 \times 10^8$  s. A stacked structure with 4-nm-thick SiO<sub>2</sub>, 2-nm-thick Al-rich Al<sub>2</sub>O<sub>3</sub>, and 10-nm-thick Al<sub>2</sub>O<sub>3</sub> could be fabricated from the viewpoint of aspect ratio even when the memory cell size is 10-nm square.

#### 4. Conclusion

In summary, we fabricated Al<sub>2</sub>O<sub>3</sub>/Al-rich Al<sub>2</sub>O<sub>3</sub>/SiO<sub>2</sub> thin film using thermal oxidation and RF magnetron co-sputtering. We clarified experimentally that the maximum capacitance in the C-V hysteresis agrees well with the series capacitance of insulators and that the minimum capacitance agrees well with the series capacitance of the semiconductor depletion layer and stacked insulator. When the Al content in the Al-rich Al<sub>2</sub>O<sub>3</sub> is increased, a large charge trap density is achieved; it is 2.6 times larger than that of the conventional trap memory. The proposed fabrication method uses only two elements (Al and O atoms) on the tunnelling insulator (SiO<sub>2</sub>), which might be suitable for fabricating nanostructures because of the simple gate structure. Moreover, the bit cost for memory devices made in this way might be very low compared with other methods because only Al and O atoms need to be prepared. The device structure would be promising for low-cost nonvolatile memory.

## References

- [1] *Single Charge Tunneling*, edited by H. Grabert and M. H. Devoret, Plenum, New York, 1992.
- [2] S. Nakata, Phys. Rev. B 47 (1993) 1679.
- [3] C.H. Lee, K. I. Choi, M. K. Cho, Y. H. Song, K. C. Park and K. Kim, Tech. Dig. Int. Electron Devices Meet., 2003, pp. 613.
- [4] C.H. Lee, K. C. Park, and K. Kim, Appl. Phys. Lett. 87 (2005) 073510.
- [5] M. Specht, H. Reisinger, F. Hofmann, T. Schulz, E. Landgraf, R. J. Luyken, W. Rösner, M. Grieb, and L. Risch, Solid State Electron., 49 (2005) 716.
- [6] S. Nakata, K. Saito and M. Shimada, IEE Electron. Lett. 41 (2005) 721.
- [7] S. Nakata, K. Saito, and M. Shimada, Appl. Phys. Lett. 87 (2005) 223110.
- [8] S. Nakata, K. Saito, and M. Shimada, Jpn. J. Appl. Phys. 45 (2006) 3176.
- [9] S. Nakata, S. Nagai, M. Kumeda, T. Kawae, A. Morimoto, and T. Shimizu, J. Vac. Sci. Technol. B 26 (2008) 1373.
- [10] D. A. Buchanan, E. P. Gusev, E. Cartier, H. Okorn-Schmidt, K. Rim, M. A. Gribelyuk, A. Mocuta, A. Ajmera, M. Copel, S. Guha, N. Bojarczuk, A. Callegari, C. D'Emic, P. Kozlowski, K. Chan, R. J. Fleming, P. C. Jamison, J. Brown, and R. Arndt, Tech. Dig. Int. Electron Devices Meet., 2000, pp. 223.
- [11] E. P. Gusev, D. A. Buchanan, E. Cartier, A. Kumar, D. DiMaria, S. Guha, A. Callegari, S. Zafar, P. C. Jamison, D. A. Neumayer, M. Copel, M. A. Gribelyuk, H. Okorn-Schmidt, C. D'Emic, P. Kozlowski, K. Chan, N. Bojarczuk, L-A. Ragnarsson, P. Ronsheim, K. Rim, R. J. Fleming, A. Mocuta, and A. Ajmera, Tech. Dig. Int. Electron Devices Meet., 2001, pp. 451.
- [12] F. R. Libsch and M. H. White, Solid State Electron., 33 (1990) 105.
- [13] J. Robertson, J. Vac. Sci. Technol. B 18 (2000) 1785.

- [14] T. Sugizaki, M. Kobayashi, M. Ishida, H. Minakata, M. Yamaguchi, Y. Tamura, Y. Sugiyama, T. Nakanishi, and H. Tanaka, Symposium on VLSI Technology, 2003, pp. 27.
- [15] V. V. Afanas'ev, M. Houssa, A. Stesmans, and M. M. Heyns, Appl. Phys. Lett. 78 (2001) 3073.
- [16] Y. Jin, K. Saito, M. Shimada, and T. Ono, J. Vac. Sci. Technol. B 21 (2003) 942.
- [17] Z. Liu, T. P. Chen, Y. Liu, M. Yang, J. I. Wong, and Z. H. Cen, Appl. Phys. Lett. 96 (2010) 173110.
- [18] S. M. Sze, Physics of Semiconductor Devices, second edition, John Wiley and Sons, New York, 1981.
- [19] S. Minami, and Y. Kamigaki, IEEE Trans. Electron Devices, ED-38 (1991) 2519.

**Figure captions:**

Fig. 1. Memory structure fabricated by RF magnetron co-sputtering:

(a) Cross section and (b) energy band diagram.

Fig. 2. RF magnetron co-sputtering method: (a) Cross-sectional view and (b) top view.

Fig. 3. Characteristics of the Al-rich Al<sub>2</sub>O<sub>3</sub> sample: (a) Al content as a function of the areal ratio of Al metals on Al<sub>2</sub>O<sub>3</sub> target and (b) leakage current density of the fabricated sample with Al content of 50%.

Fig. 4. C-V characteristics of the single Al-rich Al<sub>2</sub>O<sub>3</sub> layer with Al content of 50%.

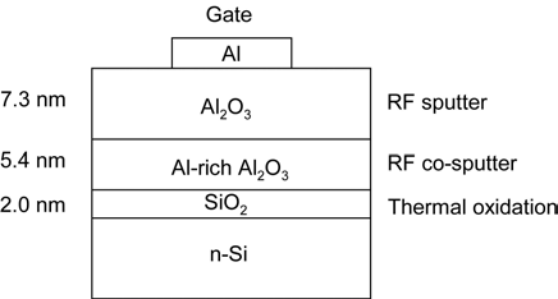
Fig. 5. C-V characteristics of the sample in Fig. 1 with Al content of 50%.

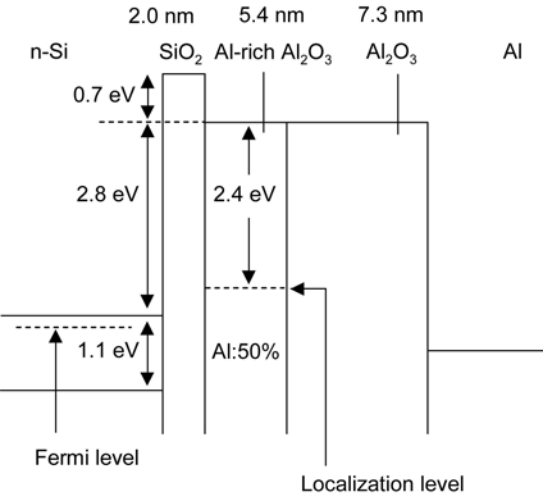
Fig. 6. Hysteresis window in voltage  $\Delta V$  as a function of (a) the hysteresis window in capacitance  $\Delta C$  and (b) the maximum applied gate voltage for the sample in Fig. 1 with Al content of 50 %.

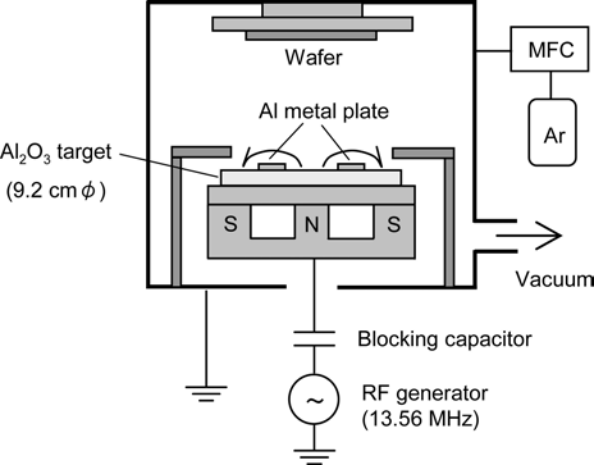
Fig. 7. Charge trap density as a function of Al content for samples with various Al-rich Al<sub>2</sub>O<sub>3</sub> layers.

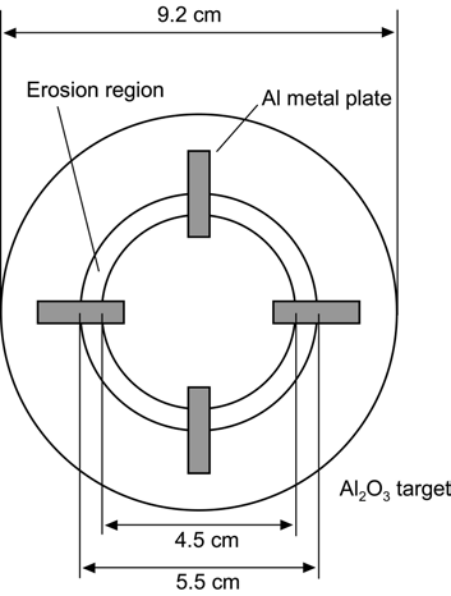
Fig. 8. Data retention characteristics for the sample with Al content of 50 %.

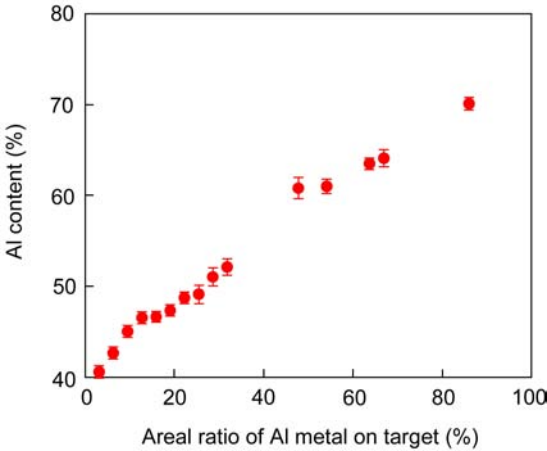
Fig. 9. Data retention characteristics for the sample with Al content of 58 %.

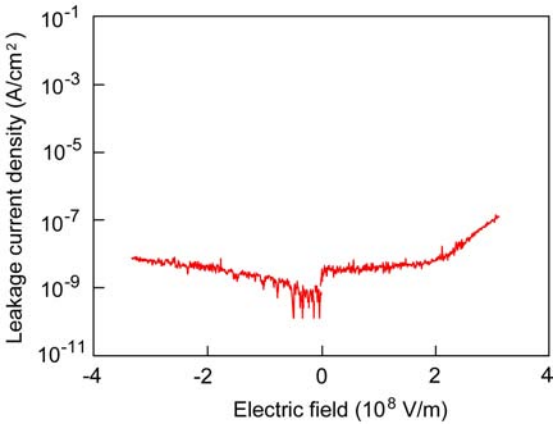


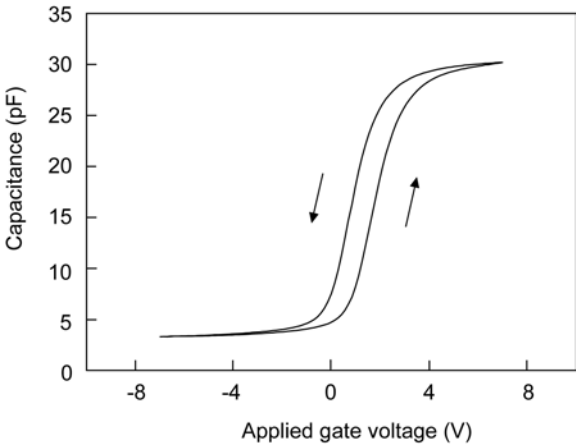


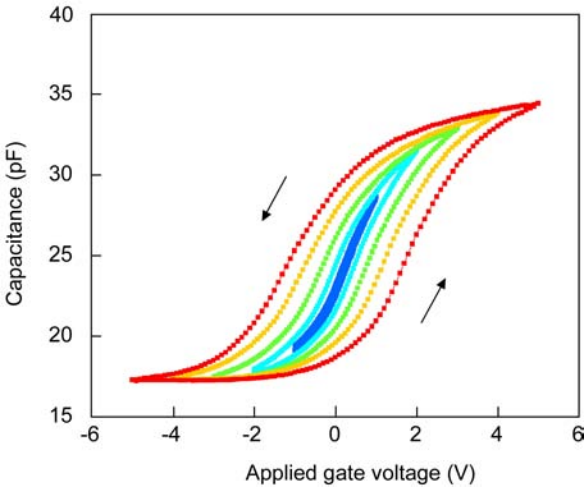


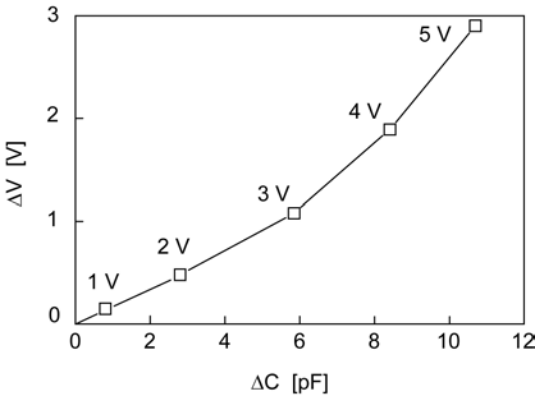


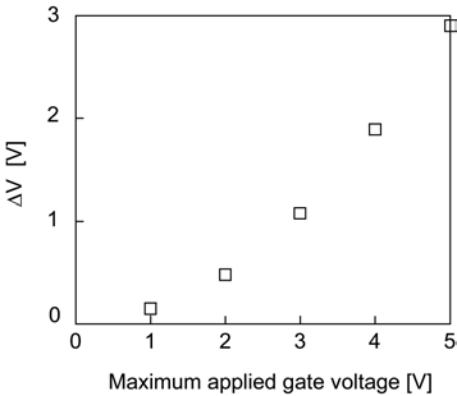


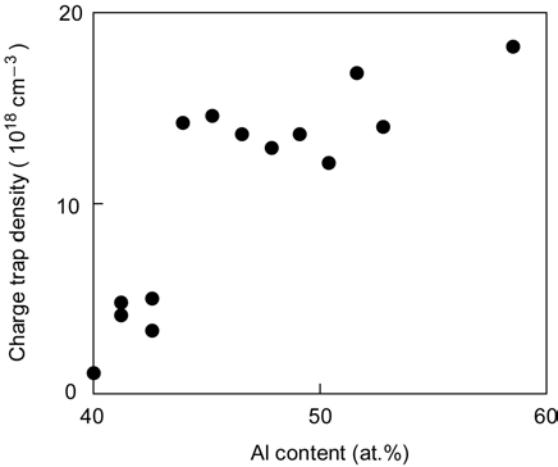


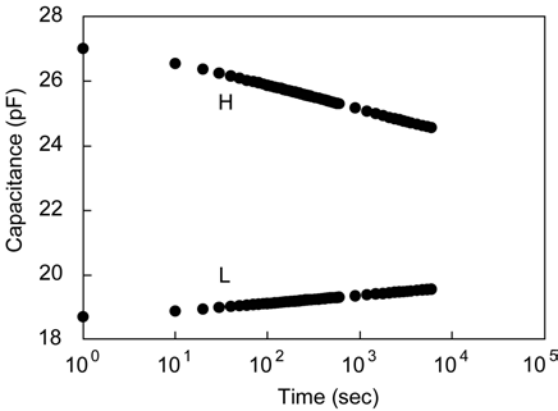


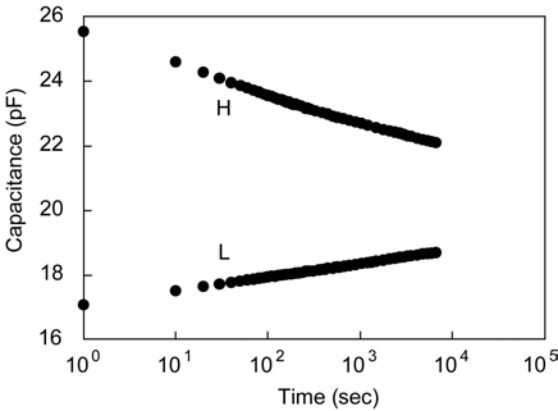












Q1, Q2 No problem

L20 Silicon

L216  $C_{Al_2O_3}$  are

L222  $C_{Al_2O_3}$

L254 metal–nitride–oxide–

L265 10–nm square

L267 silicon–oxide–

L268 nitride–oxide–silicon

L299 10–nm square

L348 second edition,